

# Analytical Modeling of Wave Fields at Extremely Long Distances and Experimental Research of Water Waves

V. Yu. Burmin and A. G. Fat'yanov

*E-mail: fat@nmsf.sccc.ru*

*Schmidt Institute of Physics of the Earth, Russian Academy of Sciences,  
ul. Bol'shaya Gruzinskaya 10, Moscow, 123995 Russia*

*Institute of Computational Mathematics and Mathematical Geophysics,  
Siberian Division, Russian Academy of Sciences, Novosibirsk, Russia*

Received April 21, 2008

**Abstract**—The analytical algorithm developed in this work is intended for modeling wave fields at extremely long distances; it has no limitations on accuracy, media models, and observation databases and makes it possible to calculate the dynamics of individual waves (primary waves, ghost waves, etc). Comparison with experimental marine data is performed with a program developed for the calculation of wave fields. The modeling performed shows that the incorporation of absorption in the Earth ensures a good agreement between the model and the observed wave fields. The formula for the ratio between waves of different multiplicities corroborated by experimental and mathematical modeling data is obtained to a first approximation for large source-receiver separation. An analytical modeling of full wave fields has been performed, some types of waves are analyzed, and the physics of multiple waves in a layer of water is studied numerically

PACS numbers: @

DOI: 10.1134/S1069351309040041

## INTRODUCTION

The study of the Earth's interior by seismic methods yields the most reliable data on its inner structure. This holds true especially for large-scale structural elements such as the whole Earth as well as for continental and oceanic regions. However, if there is demand for detailed ideas on the structure of a region, the problem is complicated by the ambiguity of the interpretation of the wavefield. Depending on the interpretation of the first and subsequent phases of (refracted, reflected, and converted) seismic waves on a seismogram, the interpreter obtains the corresponding velocity section. Unfortunately, insufficient attention has been paid to these problems lately and this has led to knowingly erroneous results. Only a few works can be noted, in which special attention was paid to the wavefield's interpretation. First of all, Tulina et al. [2003, 2006] showed how the identification of different phases of seismic waves affects the results of the interpretation of deep seismic sounding data (DSS) in marine exploration and Burmin [2004] discussed the origin of the so-called precursory waves traveling in the Earth's core. According to these works, the analysis of the recorded wave fields is a crucial stage of interpretation. Incomplete accounts of information contained in the wave fields results in an erroneous interpretation of the

waves' origins and, consequently, errors in the parameters of the velocity sections.

The ambiguity of the wavefield's interpretation is related to different factors, of which the main factors are (a) an inexperienced interpreter, (b) the complex structure of the region of the study, and (c) special features of the physics of seismic wave propagation in different elastic media. Data extracted from marine surveys, in particular, through the deep seismic sounding (DSS) method, occupy a highly important place in the interpretation of wave fields. A special feature of marine surveys concerns the specific noises—such as the reverberation of waves, resonance waves, repeated shocks, and multiple acoustic waves arising in surveys using methods of refracted as well as reflected waves—which are absent from land surveys. The wave pattern may be distorted by these noises to such an extent that the interpretation of the subsequent part of a seismogram becomes impossible or can lead to erroneous conclusions on the interior part of the Earth.

The major part of these phenomena has been studied long ago and in detail in geophysical literature [Epinat'eva, 1951; Neprochnov, 1959; Zverev, 1964] as well as in hydroacoustic literature [Cole, 1948; Bergmann et al., 1955]. Multiple acoustic waves occurring in a deep sea as a result of explosions near the surface have

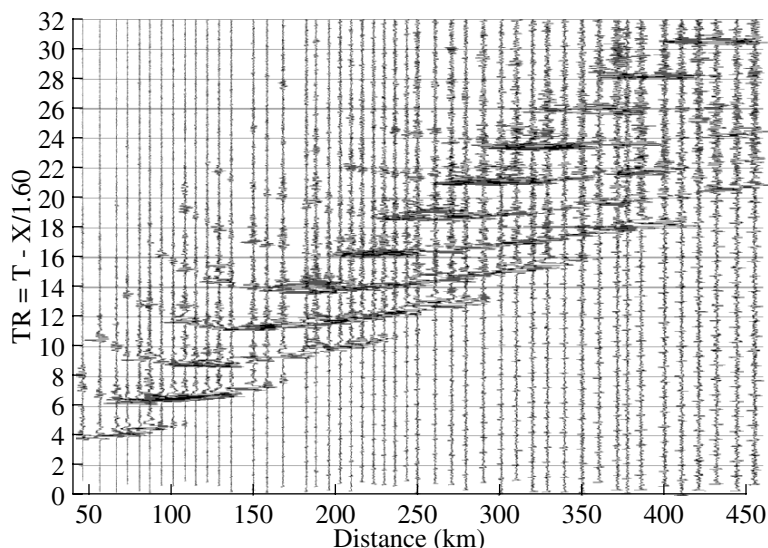


Fig. 1. The result of an experiment reduced to 1.6 km/s.  $u_z$ -component.

received significantly less attention. In this case, a pulsating sphere of a small radius (point source) having a uniform directivity diagram is considered as a source. If the source is located at a finite distance from the water surface, the so-called imaginary source arises due to the reflection of an acoustic wave from the water's surface [Brekhovskikh and Lysanov, 2007]. As a result, we have a source with a narrow-beam radiation characteristic instead of an undirected source and multiple waves reflected from the bottom of the sea, whose amplitude increases with respect to the preceding multiples with the distance from the source. By way of illustration of the latter circumstance, we present a record section presentation for water waves obtained during work conducted using the DSS method in the Atlantic ocean [Glubinnoe ... , 1996] (Fig. 1). Record section presentations are shown in this figure for the vertical displacement component of water waves produced by shallow explosions and recorded by an ocean-bottom seismograph located at a depth of about 5400 m. The explosions were detonated alternately with charges of 405 and 135 kg at a depth of 190 and 165 m, respectively. Each trace in the aforementioned construction is normalized to the maximum amplitude and multiple waves are seen distinctively in addition to the direct wave. The characteristic feature of these records is an increase in the amplitude of an acoustic wave for the first multiplicities with respect to the amplitude of the direct wave and preceding multiplicities.

The numerical modeling of the full wavefield performed in this work yields a sufficiently good representation of the observed wavefield. We analyzed certain types of waves, and numerically studied the physics of multiple waves in a water layer.

FORMULATION OF THE MODELING PROBLEM

The problem of wavefield modeling is formulated in the Cartesian coordinate system as follows. It is required to determine the components of the displacement vector for an inelastic transversally isotropic medium, which satisfy the following system of equations

$$\begin{aligned} \frac{\partial \sigma_x}{\partial x} + \frac{\partial \tau_{xy}}{\partial y} + \frac{\partial \tau_{xz}}{\partial z} &= \rho \frac{\partial^2 u_x}{\partial t^2} + F_x f(t), \\ \frac{\partial \tau_{xy}}{\partial x} + \frac{\partial \sigma_y}{\partial y} + \frac{\partial \tau_{yz}}{\partial z} &= \rho \frac{\partial^2 u_y}{\partial t^2} + F_y f(t), \\ \frac{\partial \tau_{xz}}{\partial x} + \frac{\partial \tau_{yz}}{\partial y} + \frac{\partial \sigma_z}{\partial z} &= \rho \frac{\partial^2 u_z}{\partial t^2} + F_z f(t), \end{aligned} \tag{1}$$

with the initial conditions at  $t = 0$

$$u_x = \frac{\partial u_x}{\partial t} = u_y = \frac{\partial u_y}{\partial t} = u_z = \frac{\partial u_z}{\partial t} = 0, \tag{2}$$

and boundary data at  $z = 0$

$$\sigma_z = \tau_{xz} = \tau_{yz} = 0. \tag{2'}$$

It is assumed that the components of the stress and strain tensors are related by the following well-known relations:

$$\begin{pmatrix} \sigma_x \\ \sigma_y \\ \sigma_z \\ \tau_{yz} \\ \tau_{xz} \\ \tau_{xy} \end{pmatrix} = \begin{bmatrix} C_{11} & C_{12} & C_{13} & 0 & 0 & 0 \\ C_{12} & C_{11} & C_{13} & 0 & 0 & 0 \\ C_{13} & C_{13} & C_{33} & 0 & 0 & 0 \\ 0 & 0 & 0 & C_{44} & 0 & 0 \\ 0 & 0 & 0 & 0 & C_{44} & 0 \\ 0 & 0 & 0 & 0 & 0 & \frac{1}{2}(C_{11} - C_{12}) \end{bmatrix} \begin{pmatrix} \epsilon_x \\ \epsilon_y \\ \epsilon_z \\ \epsilon_{yz} \\ \epsilon_{xz} \\ \epsilon_{xy} \end{pmatrix}.$$

Note that components of the strain tensor are defined in terms of the components of the displacement vector as follows:

$$\begin{aligned}\varepsilon_x &= \frac{\partial u_x}{\partial x}, & \varepsilon_y &= \frac{\partial u_y}{\partial y}, & \varepsilon_z &= \frac{\partial u_z}{\partial z}, \\ \varepsilon_{yz} &= \frac{\partial u_y}{\partial z} + \frac{\partial u_z}{\partial y}, & \varepsilon_{xz} &= \frac{\partial u_x}{\partial z} + \frac{\partial u_z}{\partial x}, \\ \varepsilon_{xy} &= \frac{\partial u_x}{\partial y} + \frac{\partial u_y}{\partial x}.\end{aligned}$$

The algorithm for calculating waves in an anisotropic inelastic media is based on the Volterra relations taking into account the influence of the elastic aftereffect. Namely, the elastic constants  $c_{ij}$  are replaced by the integral operators  $C_{ij}$  [Fat'yanov, 1989]

$$C_{ij}x = c_{ij}x(t) - c'_{ij} \int_{-\infty}^t h_{ij}(t-\tau)x(\tau)d\tau. \quad (3)$$

where  $c'_{ij}$  are quantities determining the absorption level. The aftereffect function (of the core) determined the spectral composition of absorption. The physical parameters of absorption (absorption decrements or damping factor  $Q$  of  $P$  and  $S$  waves) are determined from  $c'_{ij}$  [Fat'yanov, 1989]. The components of the force vector  $F_x$ ,  $F_y$ , and  $F_z$  describe concentrated sources of various types.

The special choice of the components of the force vector makes it possible to also incorporate sources of the type of the seismic momentum tensor. For this it is sufficient to give, e.g.,  $F_x$  in the following form:

$$\begin{aligned}F_x &= M_{xx}\delta'(x-x_0)\delta(y-y_0)\delta(z-z_0) \\ &+ M_{xy}\delta(x-x_0)\delta'(y-y_0)\delta(z-z_0) \\ &+ M_{xz}\delta(x-x_0)\delta(y-y_0)\delta'(z-z_0).\end{aligned} \quad (4)$$

Here,  $M_{ij}$  are components of the seismic momentum tensor [Aki and Richards, 2002]. In the case of a source of the seismic momentum tensor type, the components  $F_y$  and  $F_z$  of the force vector are given in the same way. Fat'yanov [1991] obtained a solution of problem (1), (2), and (2') for layered anisotropic inelastic media in the case of a source of the seismic momentum tensor type.

In this work the emphasis is on the algorithm for computation and modeling of wave fields in an elastic-fluid media consisting of a fluid layer lying on an arbitrary number of anisotropic inelastic layers, which is applicable to the analysis of marine survey data.

## METHOD OF MATHEMATICAL MODELING

There are a number of numerical methods of calculating wave fields in layered media. It is impossible to list all these works in this paper. We note [Smirnov and Sobolev, 1932; Petrashen', 1957; Zvolinskii, 1957; Samarskii, 1977; Alekseev and Mikhailenko, 1978; Kononov, 1979]. All these methods have their own field of application and can calculate only the full wavefield without extracting an individual type of wave. At the same time, algorithms making it possible to calculate the dynamics of individual waves are of great and often primary importance in problems of the modeling of wave fields in complexly structured media. The asymptotic ray-tracing method is the only method of numerical analysis of a wavefield in parts. However, there are well-known limitations on its application. Below we describe the semi-analytical method of calculating a full field and individual types of waves (primary, multiple, ghost waves, etc) in layered media with an arbitrary number of layers based on a special expansion of the exact solutions and free from the limitation of the ray-tracing method. Note that the explicit formulas obtained in the spectral region make it possible to perform calculations at extremely long distances for arbitrary models of a medium without any limitations.

The fluid medium is considered as a particular case of the elastic medium, in which  $\mu = 0$  and  $v_s = 0$  [Molotkov, 1984]. The following characteristics of an elastic medium are used for the description of the fluid state: the displacement vector  $\mathbf{u}$  and the  $\sigma_{zz}$ -component of the stress tensor. Transition to the conventional characteristic of a fluid, i.e., pressure  $p$ , is performed in the well-known manner, i.e.,  $p = -\sigma_{zz}$ .

Below we consider an axially symmetric source of the type of the "expansion center" with to the aim of performing a practical implementation of the method. In this case, in the cylindrical coordinate system, only components  $u_r(r, z, t)$  and  $u_z(r, z, t)$  are nonzero. The boundary conditions at the surface of the water and at the fluid-earth interface have the form [Molotkov, 1984]

$$\sigma_{zz}|_{z=0} = 0,$$

$$[u_z] = [\sigma_{zz}] = \tau_{rz}^-|_{z=h} = 0. \quad (5)$$

Here  $z = 0$  is the fluid free surface,  $z = h$  is the bottom depth, and the jump  $[a] = a^- - a^+$ , where  $a^+$  is the value of  $a$  at  $z = h$  on the fluid side and  $a^-$  is the value of  $a$  at  $z = h$  on the solid body side.

Below we use the Fourier-Bessel transform over variables  $(r, t)$  for the solution's construction and a transfer is carried out to the potentials  $\varphi$  and  $\psi$  of the  $P$  and  $S$  waves in the spectral region:

$$u_r = -k\varphi - \frac{d\psi}{dz} = -k\varphi, \quad u_z = \frac{d\varphi}{dz} + k\psi = \frac{d\varphi}{dz},$$

$$\sigma_{zz} = \lambda \frac{du_z}{dz} + k\lambda u_r = -\rho\omega^2\phi = -p. \tag{6}$$

Determination of the potential  $\phi$  and, consequently, all the sought components of the field from (6) is performed by a semi-analytical method [Fat'yanov, 1990, 2005].

We describe its main stages as applied to obtaining a solution in a fluid layer. The function  $\alpha$  satisfying the following condition at  $z = h$

$$\frac{d\phi^+}{dz} = \alpha\phi^+. \tag{7}$$

is easily obtainable with the use of the semi-analytical method.

Then, making use of (5) and (6), we obtain, for example, the vertical component of the displacement  $u_z$  at an arbitrary position of the source  $d > 0$  and receiver  $z$

$$\begin{aligned} &u_z(z, k, \omega) \\ &= \frac{F(\omega)}{4\pi c^2} \left\{ \frac{e^{-v|z-d|} + qe^{-v(2h-z-d)}}{1 + qe^{-2vh}} \right\} (1 + e^{-2vz}) \\ &\quad \text{при } z < d, \\ &u_z(z, k, \omega) \\ &= \frac{F(\omega)}{4\pi c^2} \left\{ \frac{e^{-2vd} + qe^{-2v(h-d)}}{1 + qe^{-2vh}} \right\} \text{при } z = d, \tag{8} \\ &u_z(z, k, \omega) \\ &= \frac{F(\omega)}{4\pi c^2} \left\{ \frac{-e^{-v(z-d)} + qe^{-v(2h-z-d)}}{1 + qe^{-2vh}} \right\} (1 - e^{-2vz}) \\ &\quad \text{при } z > d. \end{aligned}$$

Here  $v = \sqrt{k^2 - \omega^2/c^2}$ ,  $c$  is the velocity of sound in fluid,  $q = (v - \alpha)/(v + \alpha)$  is the spectral reflection coefficient taking into account the properties of the fluid and solid earth, and  $F(\omega)$  is the spectrum of the input signal  $f(t)$  (see 1).

Expressions for the pressure  $p$  and the component  $u_r$  have the form

$$\begin{aligned} &p(z, k, \omega) \\ &= \rho \frac{F(\omega)\omega^2}{4\pi c^2 v} \left\{ \frac{e^{-v|z-d|} + qe^{-v(2h-z-d)}}{1 + qe^{-2vh}} \right\} (1 - e^{-2vz}), \tag{9} \\ &u_r(z, k, \omega) \end{aligned}$$

$$= -\frac{F(\omega)k}{4\pi c^2 v} \left\{ \frac{e^{-v|z-d|} + qe^{-v(2h-z-d)}}{1 + qe^{-2vh}} \right\} (1 - e^{-2vz}). \tag{10}$$

As can be seen from (8), the reciprocity principle is inapplicable to the component  $u_z$ , while the reciprocity principle holds for the horizontal component and pressure [Brekhovskikh and Godin, 1989].

Let us analyze formula (8) as applied to experimental data (the receiver is on the bottom ( $z = h$ )). The term  $-e^{-2vd}$  yields a ghost wave from a source. The denominator in (8)--(10) can be represented in the form

$$\begin{aligned} &\frac{1}{1 + qe^{-2vh}} \\ &= 1 - qe^{-2vh} + q^2e^{-4vh} + \dots + (-1)^n q^n e^{-2vhn} + \dots \end{aligned} \tag{11}$$

The analysis of the summands in (11) with respect to the Sommerfeld formula shows that they yield arbitrary multiplicities in the general solution. Substitution of representation (11) into (8)--(10) yields the expansion of the sought solution for a fluid layer in the sum of waves of an arbitrary multiplicities.

For clarity's sake, we consider only the first term in (11) (multiples are absent). In this case, if  $z = h > d$  (receiver at the bottom), (8) takes the form

$$\begin{aligned} u_z(z, k, \omega) &= u_z^0(z, k, \omega) = -\frac{F(\omega)}{4\pi c^2} e^{-v(h-d)} \\ &+ \frac{F(\omega)}{4\pi c^2} q e^{-v(h-d)} + \frac{F(\omega)}{4\pi c^2} (1-q) e^{-v(h+d)}. \end{aligned} \tag{12}$$

The first term in (12) represents a direct wave from a source in the spectral region and the second term represents the direct wave with respect to its interaction with the bottom. The third term represents a ghost wave with respect to its interaction with the bottom. Representation (12) makes it possible to take into account the interaction with the bottom separately for the direct and ghost waves. Subtraction of terms of the form  $qe^{-v(h-d)}$  from (12) is sufficient for this and will be used in wave pattern analysis.

Now we address two terms in expansion (11) and represent the denominator in (8) in the form

$$\frac{1}{1 + qe^{-2vh}} = 1 - qe^{-2vh}. \tag{13}$$

The substitution of (13) into (8) yields the following expression for the field

$$u_z(z, k, \omega) = u_z^0(z, k, \omega) + u_z^1(z, k, \omega), \tag{14}$$

$$\begin{aligned} u_z^1(z, k, \omega) &= \frac{F(\omega)}{4\pi c^2} q(1-q)e^{-v(3h-d)} \\ &- \frac{F(\omega)}{4\pi c^2} q(1-q)e^{-v(3h+d)}. \end{aligned} \tag{15}$$

In (15),  $u_z^1$  is a primary wave consisting of a direct primary wave from the source and a primary ghost wave. The representation of the solution in the form of the sum of multiple waves can be obtained with respect to expansion (11) in the same way. It is an easy matter to extract a wave of arbitrary multiplicity from the solution, remove the ghost waves, consider the interaction of direct waves with the bottom, etc.

We obtain all the sought components of the wavefield in the physical region  $(z, r, t)$  using the inverse Fourier-Bessel transform.

#### SCHEME OF THE EXPERIMENT AND THE RESULTS OF THE MODELING OF THE WAVEFIELD

The adopted scheme of the numerical experiment was closest to that of the field experiment conducted in the Atlantic Ocean on the Angola-Brazil geotraverse in 1986 [Glubinnoe ..., 1996]. The bottom seismic station was deployed in the Brazil Basin and explosions were detonated along the profile in the E--W direction at about 50-km intervals. The sea depth at the station is about 5400 m. The model of the medium was taken from DSS data and consists of six layers.

This algorithm was programmed and the program makes it possible to simulate a full wave fields as well as individual fragments of the wavefield. Full wave fields of the vertical displacement component and pressure are shown for the sought model of the medium in the absence of absorption in Figs. 2a, 2b. The initial source-receiver separation was 50 m and the distance between sources was 8.511 km, the source was submerged at a depth of 190 m, which concurs with the field experiment. The results of the calculations were outputted every 10 ms. For comparison with real data, we constructed a record section reduced to a velocity of 1.6 km/s and normalized each trace to the maximum amplitude. Record sections are shown in Figs. 3a and 3b for the vertical component of displacement and pressure. Comparison between Figs. 1 and 3a shows that they differ significantly from each other although they were constructed in the same way. Thus, we failed to reach agreement of the observed data with the model results in the framework of an elastic model. We will show below that the incorporation of absorption in the solid Earth makes it possible to obtain a strong agreement of the observed data with the results of the modeling.

#### COMPARISON OF EXPERIMENTAL DATA AND WAVEFIELD ANALYSIS

In order to take into account the main factors affecting wavefield formation more fully, we consider the model of the medium with respect to absorption in a solid medium. Data on absorption of the  $P$  and  $S$  waves

in the region are absent, therefore we use data presented in [Kondrat'ev, 1986], which are typical of sedimentary rocks and sufficient for a qualitative description of elastic wave propagation. The full wavefield in a solid medium with absorption are presented in Figs. 4a and 4b for, respectively, the vertical displacement component and pressure, and their record sections are presented in Figs. 5a and 5b. The comparison of Fig. 5a with Fig. 1 shows strong agreement of the real data with the model results. Thus, the results of numerical modeling show that the incorporation of absorption in the Earth significantly improves the agreement of the model results with the real data.

The tendency of an increase of amplitudes of the multiple wave is traced distinctively in the real data (Fig. 1). Similar phenomena are observed in the model calculations. Note that the pattern of variation in the wave fields is nearly the same for the component  $U_z$  and pressure  $P$  (Fig. 5), i.e., the amplitude of acoustic waves of the first multiplicities becomes larger than the amplitudes of the direct wave and the wave of the preceding multiplicity.

In order to perform a more detailed study of this phenomenon, we conducted additional calculations. For clarity's sake, the simplified scheme of the experiment is presented in Fig. 6. Figure 7a shows the vertical component  $U_z$  and the pressure at the point O (Fig. 6). As can be seen from Fig. 7a, the wavefield pattern becomes ordinary in the case of normal incidence. The direct wave is recorded as the first arrival and then multiple waves are recognized distinctively. The amplitude of the direct wave is maximum and the intensity of multiple waves decrease monotonically with their multiplicity. The record section is shown in Figs. 7b and 7c for the vertical  $U_z$ -component and the pressure at points  $P$  and  $R$ . These figures show that an increase of multiple waves occurs at more distant distances from the source (the point  $R$ ).

Let us consider the main factors causing an increase in the amplitudes of multiple arrivals. The amplitude of multiple waves is determined mainly by two factors (excluding structural ones): geometric divergence and the reflection coefficient.

Taking the reflection coefficient into account can result in an increase in the wave's amplitude, for example, in a postcritical area. Because the angle of incidence decreases with the wave's multiplicity, an increase in the amplitudes of multiple waves cannot be caused by this factor. Note that the source-receiver distance in the real experiment is large and therefore angles of incidence will be confined to a postcritical area.

Let us dwell more particularly on the geometric divergence. The intensity of the  $Z$ -component of a

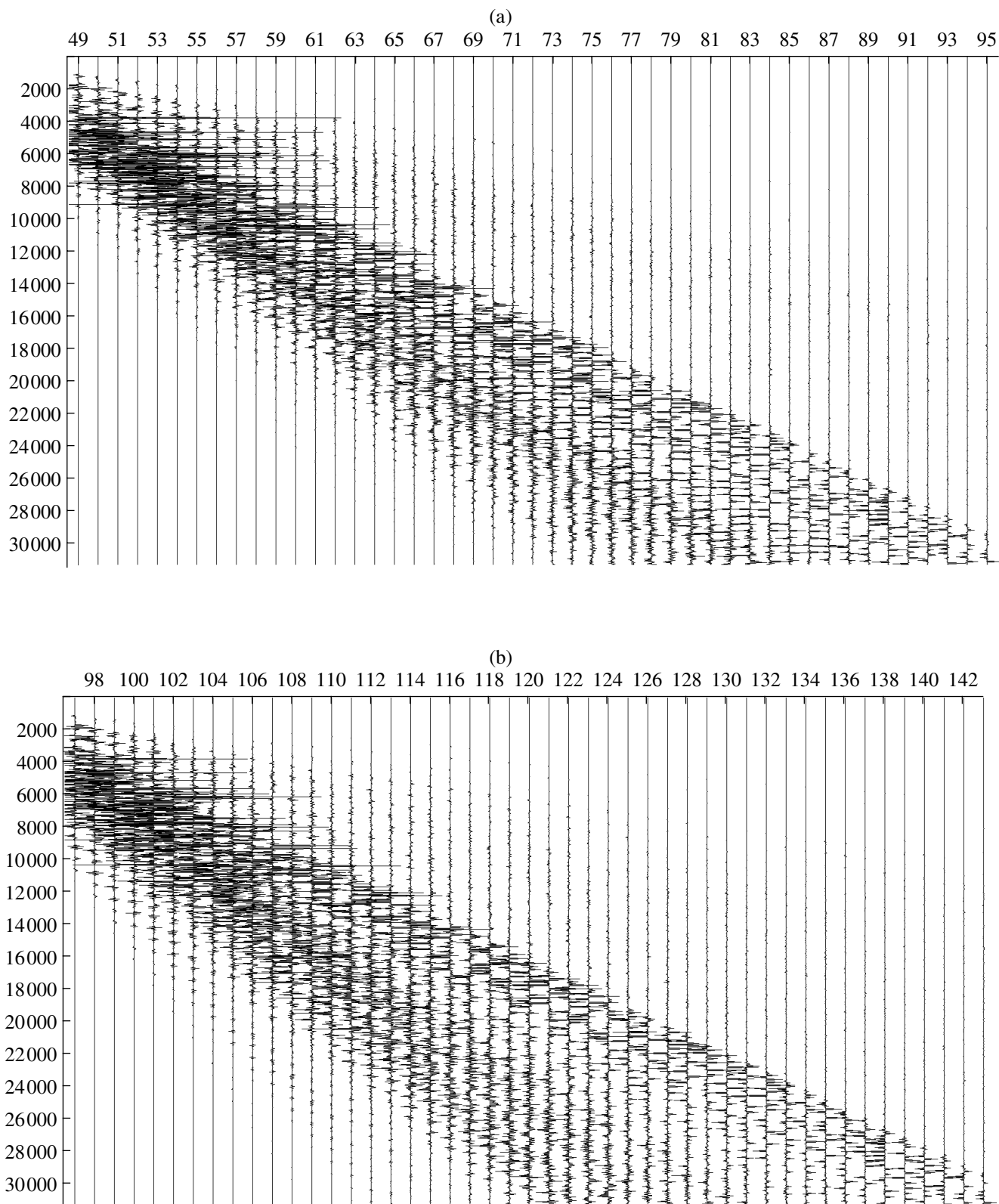


**Fig. 2.** Full wavefield: (a)  $u_z$ -component, (b) pressure  $p$ .

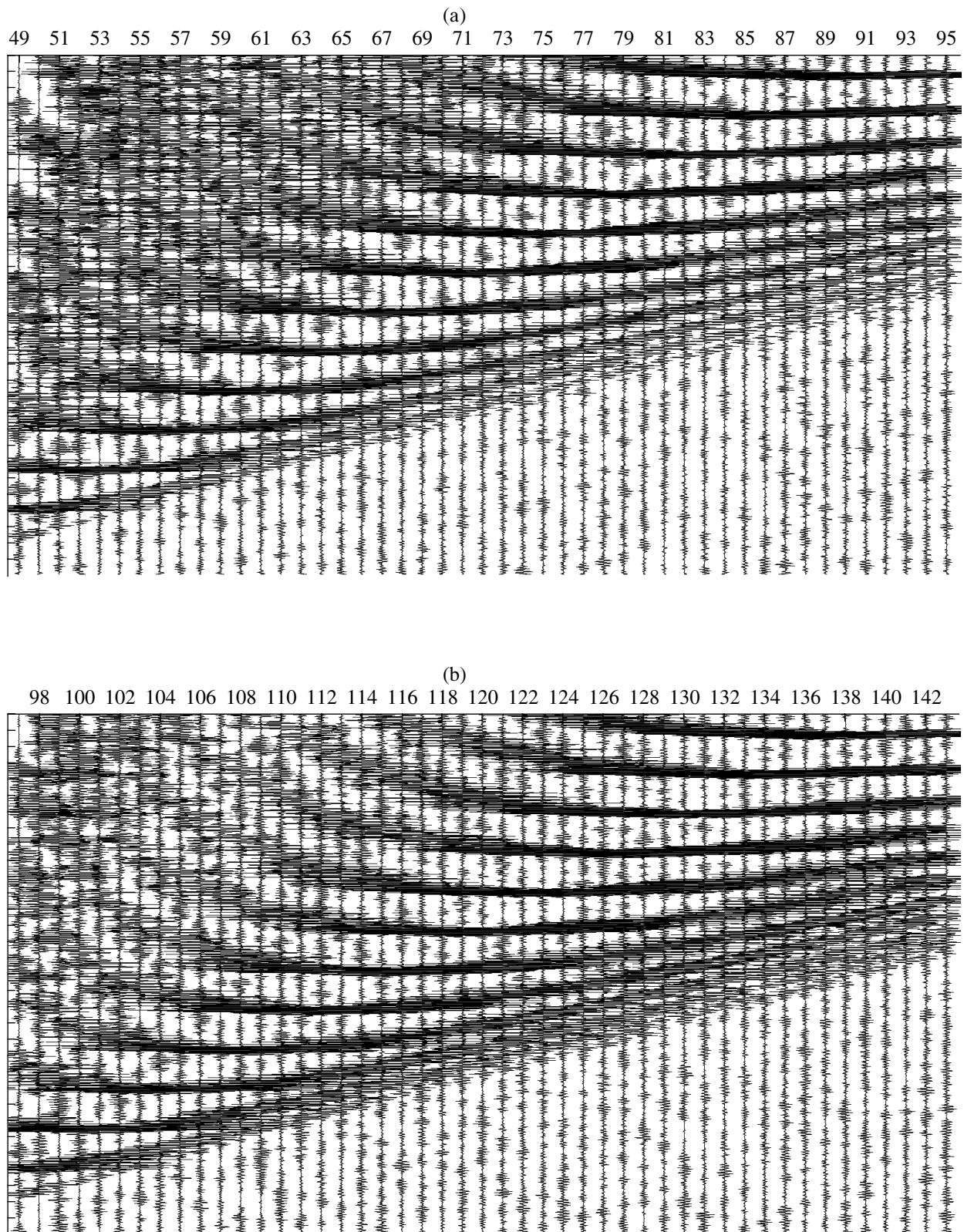


**Fig. 3.** The result of computations of (a)  $u_z$ -component and (b) pressure  $p$  reduced to 1.6 km/s.

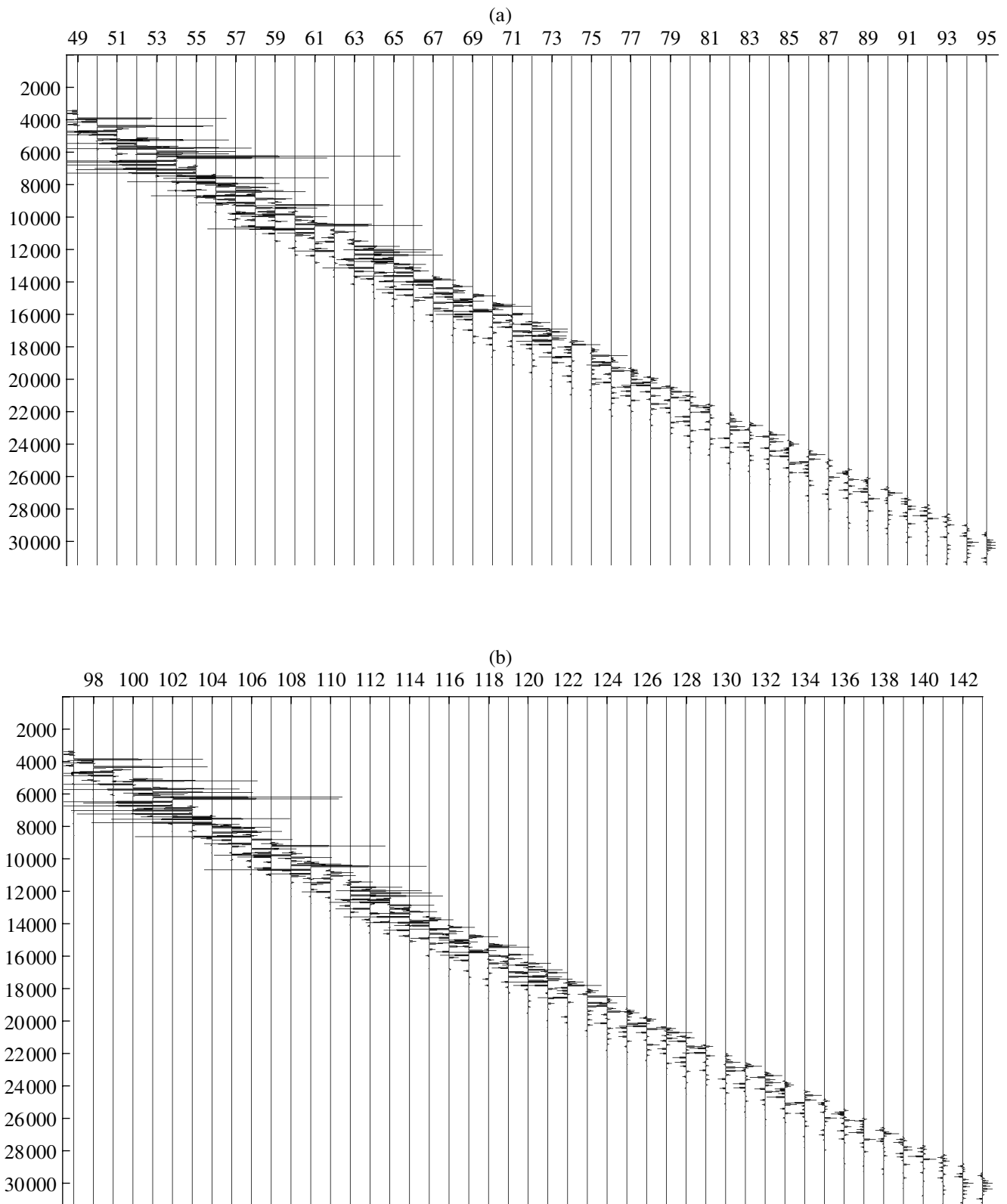


**Fig. 4.** The full wavefield with absorption: (a)  $u_z$  component and (b) pressure  $p$ .

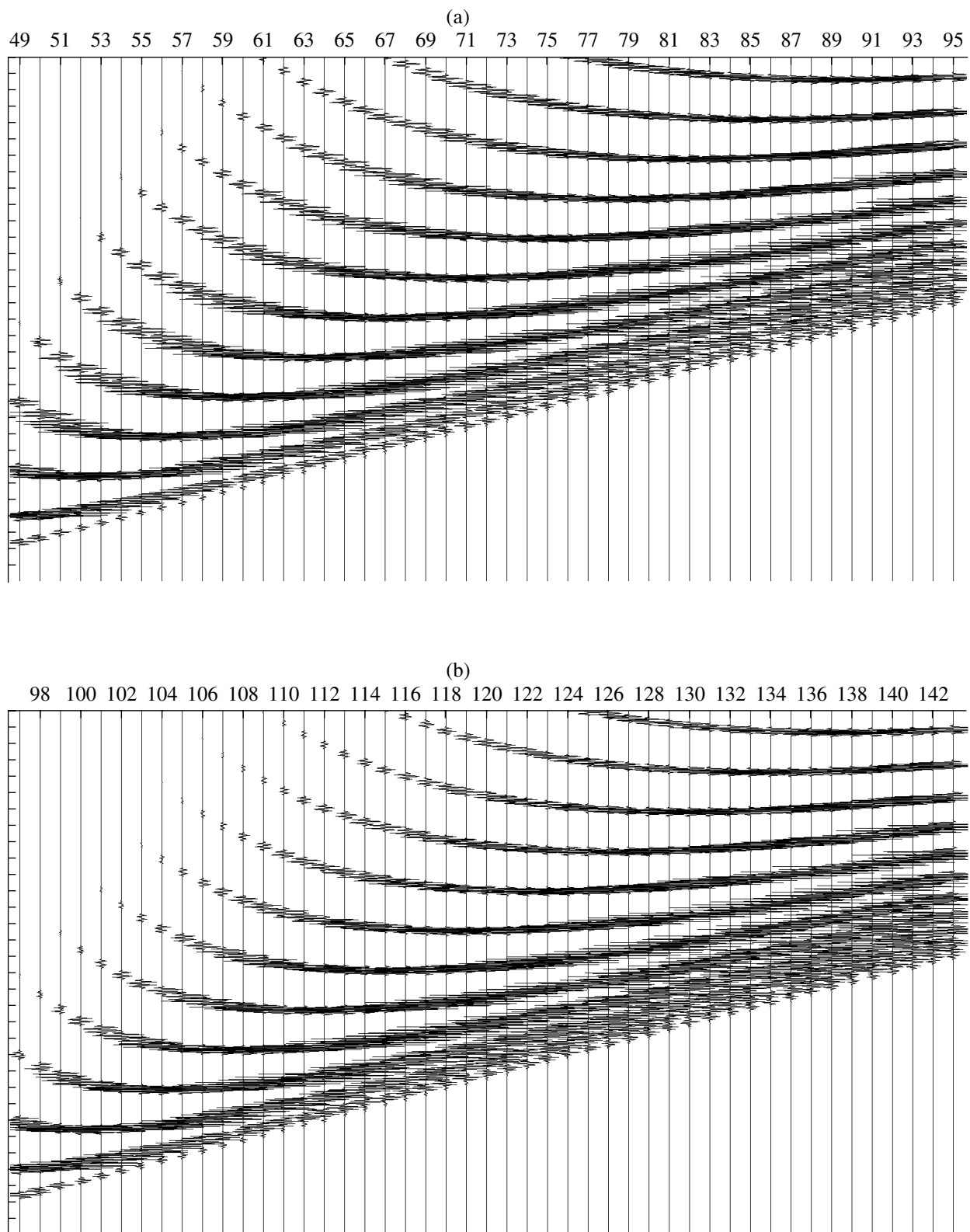


**Fig. 5.** The result of computations of (a)  $u_z$  component and (b) pressure  $p$  reduced to 1.6 km/s.

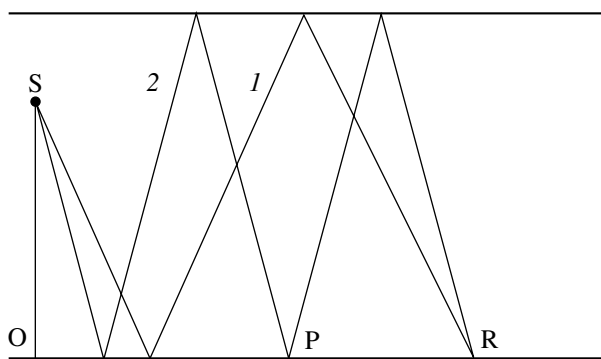


Fig. 6. Simplified scheme of the experiment.

wavefield in a far-field zone can be represented in the form [Aki and Richards, 2002]

$$u_i = c_i \frac{1}{r_i} \cos(\varphi_i). \quad (16)$$

where  $i \geq 1$  is the wave's multiplicity,  $u_i$  is the wave's intensity,  $r_i$  is the distance traveled by a wave of multiplicity  $i$ , and  $\varphi_i$  is the angle of incidence.

Neglecting the factor  $c_i$  determined by the reflection coefficient, we obtain the following approximate value for the ratio of multiple wave intensities for the  $u_z$ -component calculated at the bottom at significant, as compared with the thickness of the fluid layer, source-receiver distances

$$\frac{u_{i+1}}{u_i} = \frac{\cos(\varphi_{i+1})}{\cos(\varphi_i)}.$$

It is easy to show that

$$\cos(\varphi_i) = (h - d + 2hi)/r_i.$$

where  $h$  is the thickness of the water layer and  $d$  is a depth, at which the sources are located.

Assuming that  $r_{i+1} = r_i$  and taking into account that  $d \ll h$ , we obtain the following approximate formula for the ratio of intensities of multiples at large source-receiver distances

$$u_{i+1}/u_i = h + 2h(i + 1)/h + 2hi = (2i + 3)/(2i + 1).$$

Then, for example,

$$u_2/u_1 = 5/3 \approx 1.67. \quad (17)$$

The obtained value of the ratio (17) is supported by the data of modeling (Fig. 7b) for large source-receiver distances at point  $R$ .

Let us consider, in greater detail, the model results obtained for multiple pressure waves. As for the vertical component, an increase of multiples is also observed for them. This, however, cannot be accounted for by the geometric factor (16). This phenomenon can be accounted for in part by the occurrence of the so-called imaginary source [Brekhovskikh and Lysanov, 2007].

By way of illustration of this phenomenon, we performed calculations without ghost waves, which together with the direct wave form a special directivity diagram of the source and create a so-called imaginary source. The record section is shown in Fig. 8 for the pressure field without a ghost wave at points  $P$  and  $R$  (Fig. 6). Comparison with Fig. 7c showing the record section for a full pressure field shows that a quantitative change occurs in the wavefield pattern. However, a qualitative change does not occur, and the effect of an increase of multiples (at the point  $R$ ) remains. The results of modeling showed that the effect of an increase of multiples calculated without accounting for ghost waves remained even with sources at lesser depths. The model calculations show that an increase of the multiple waves of greater multiplicity is observed in the full field and in the field without ghost waves where the source was at a less submerged depth. For example, an increase of multiple waves in the full pressure field occurs at point  $P$  up to the 3rd multiplicity and without accounting for the imaginary source up to the 2nd multiplicity at a submergence depth of the source of 90 m.

Thus, the dipole property of the source, which is submerged at a shallow level, accounts for the effect of an increase of the pressure multiples only partly. Let us simplify the model wavefield still more. The record section is shown in Fig. 9 for pressure at the points  $P$  and  $R$  (Fig. 6) without ghost waves and without accounting for the interaction of a direct wave with the bottom. As can be seen from Fig. 9, in this case, the effect of an increase of multiple pressure waves disappears completely and they begin to decrease monotonically. This effect is observed at the source placed at a depth of 90 m. Thus, the increase of multiple pressure waves is accounted for by the occurrence of the imaginary source and the interaction of the wavefield with the bottom.

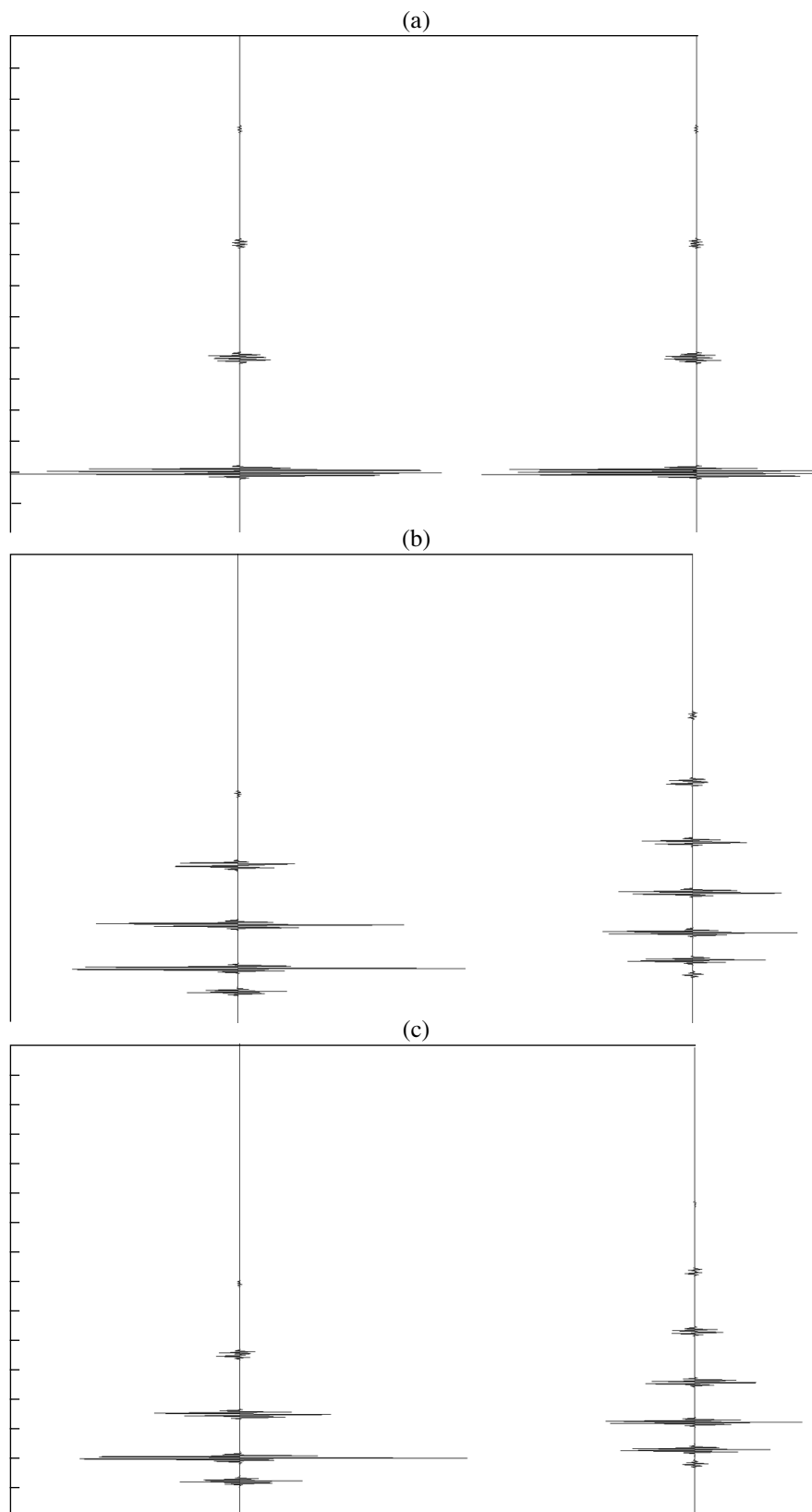


**Fig. 7.** Wave fields: (a)  $u_z$  at points O (Fig.6), (b)  $u_z$  at points  $P$  and  $R$  (Fig. 6), and (c) pressure at points  $P$  and  $R$  (Fig. 6) reduced to 1.6 km/s.

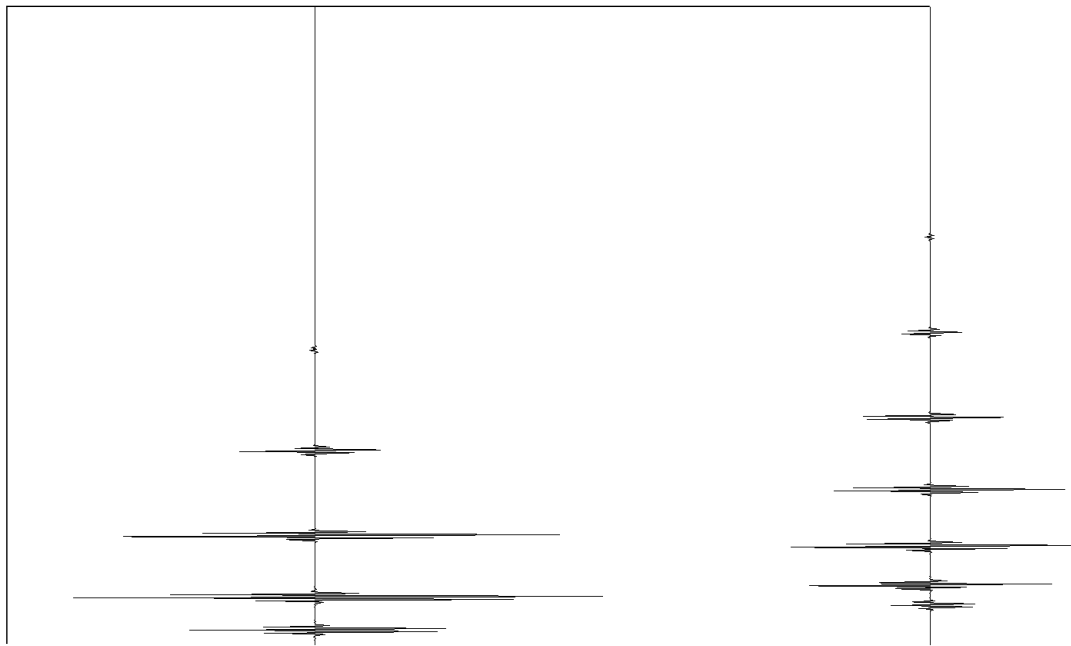


**Fig. 8.** Pressure wave fields without ghost waves reduced to 1.6 km/s at points @P and @R (Fig. 6).

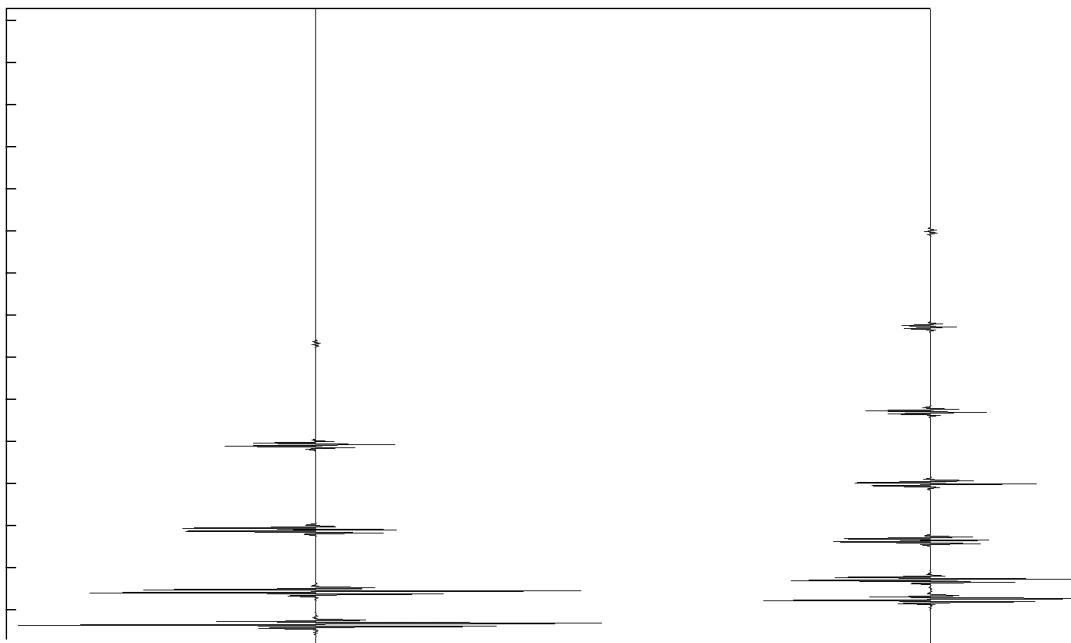


**Fig. 9.** Pressure wave fields reduced to 1.6 km at *P* and *R* points (Fig. 6) without ghost waves and interaction with bottom.

### CONCLUSIONS

An analytical algorithm for the modeling of wave fields at extremely long distances is developed in the work, which has no limitations on accuracy, media models, and observation databases and makes it possible to calculate the dynamics of individual waves (primary waves, ghost waves, etc). Comparison with marine experimental data was conducted with the pro-

gram developed for the calculation of wave fields. The modeling performed shows that the incorporation of absorption in the Earth ensures a strong agreement of the model field with the observed field. The formula for the ratio of intensities of waves of different multiplicities is obtained in a first approximation for large source-receiver distances and is corroborated by the experimental and model data. The analytical modeling of full

wave fields is performed, some types of waves are analyzed, and the physics of multiple waves in a liquid layer is studied numerically.

## REFERENCES

- K. Aki and P. Richards, *Quantitative Seismology*, 2nd ed. (Univ. Science Books, 2002).
- A.S. Alekseev and B. G. Mikhailenko, "The method of Calculation of Theoretical Seismograms for Complexly Structured Model of a Medium," *Sov. Phys. Dokl.* **240** (5) (1978)
- P. G. Bergmann et al.; *Physical Foundations of Underwater Acoustics* (Sov. Radio, Moscow, 1955) [in Russian].
- L. M. Brekhovskikh and O. A. Godin; *Acoustics of Layered Media* (Nauka, Moscow, 1989) [in Russian].
- L. M. Brekhovskikh and Yu. P. Lysanov *Theoretical Foundations of Ocean Acoustics* (Nauka, Moscow, 2007) [in Russian].
- V. Yu. Burmin, "Seismic Wave Velocities in the Earth Crust," *Fizika Zemli*, No.6, 24 (2004) [*Izvestiya, Physics of the Solid Earth* **40** (6) (2004)].
- @Deep Seismic Sounding of Lithosphere on the Angola-Brazil Geotraverse, *Ed. by S. M. Zverev, I. P. Kosminskaya, and Yu. V. Tulina* (MGK, Moscow, 1996).
- S. M. Zverev, *Seismic Studies at Sea* (Moscow State Univ., Moscow, 1996) [in Russian].
- N. V. Zvolinskii, "Reflected and Head Waves Arising at a Planar Interface," *Izv. AN SSSR, ser. Geofiz.*, No. 10. (1964)
- O. K. Kondrat'ev, *Seismic Waves in Absorbing Media* (Nedra, Moscow, 1986) [in Russian].
- A. N. Konovalov, *Numerical Solution of Problems of the Elasticity Theory in Terms of Stresses* (Novosibirsk State Univ., Novosibirsk, 1964) [in Russian].
- R. H Cole, *Underwater Explosions* (Princeton Univ. Press, Princeton, New Jersey, 1948).
- L. A. Molotkov, *Matrix Method in the Theory of Wave Propagation in Layered Elastic and Liquid Media* (Nauka, Leningrad, 1984) [in Russian]
- G. I. Petrashen', "The Method of the Solution Construction for Problems of Seismic Wave Propagation in Isotropic Media with Thick Plane-Parallel Layers," in *Voprosy Dinamicheskoi Teorii Rasprostraneniya Seismicheskikh Voln.*(Gostopizdat, Leningrad, 1957), No.1, pp. 7–69.
- A. A. Samarskii, *Theory of Finite-Difference Schemes* (Nauka, Moscow, 1977) [in Russian].
- V. I. Smirnov and S. L. Sobolev, "On a New Method in a 2-D Problem of Elastic Oscillations," *Trudy Seismologicheskogo Inst.*, No. 20, (1932).
- Yu. V. Tulina, V. Yu. Burmin, I. B. Shmeleva, and N. A. Alekseeva, "On Geological Origin of Differences in Seismic Fields along Various Directions in the Angola Basin," *Fizika Zemli*, No. 6 (2003b) [*Izvestiya, Physics of the Solid Earth* **39** (6) (2003)].
- Yu. V. Tulina, V. Yu. Burmin, and I. B. Shmeleva, "Is it Possible to Construct Velocity Section by the DSS method from Data on Seismic Waves Recorded in First Arrivals?," in *Sbornik Trudov Sed'mykh Chtenii im. A.A. Fedynskogo*, (Nauchnyi Mir, Moscow, 2006), pp. 114–128.
- A. G. Fat'yanov, *Nonstationary Seismic Wave Fields in Heterogeneous Anisotropic Media with Energy Absorption*, (Akad. Nauk. SSSR, Siberian Division, Novosibirsk, 1989).
- A. G. Fat'yanov, "Semi-analytical Method of Solving Direct Dynamic Problems in Layered Media," *Dokl. Akad. Nauk SSSR*, **310** (2), 323 (1990).
- A. G. Fat'yanov, "Forward and Inverse Problems for the Seismic Momentum Tensor in Layered Media," *Dokl. Akad. Nauk SSSR*, **317** (6), 1357 (1991).
- A. G. Fat'yanov, "Mathematical Modeling of Wave Fields in Media with Curvilinear Boundaries," *Dokl.Phys.*, **401** (4), 529 (2005).6

SPELL: 1. seismogram